Electronic Supplementary Material (ESI) for Journal of Materials Chemistry A.

Carbon layer-confined MoS_2/Ni_3S_2 heterostructure with enhanced sodium and potassium storage performance

Jin Bai,‡[a] Jianguo Si,‡[d] Yunjie Mao,[ab] Hongyang Ma,[ab] Peiyao Wang,[ab] Wanyun Li,[ab] Ke Xiao,[ab] Guofeng Zhang,[a] Yiyong Wei,[e] Xuebin Zhu,*[a] Bangchuan Zhao*[a] and Yuping Sun[ac]

[a]Key Laboratory of Materials Physics, Institute of Solid State Physics, HFIPS, Chines e Academy of Sciences, Hefei 230031, People's Republic of China

[b]University of Science and Technology of China, Hefei 230026, People's Republic of China

[c]High Magnetic Field Laboratory, Chinese Academy of Sciences, Hefei 230031, People's Republic of China

[d]Spallation Neutron Source Science Center, Institute of High Energy Physics, Chinese Academy of Sciences, Dongguan 523803, People's Republic of China

Prof. Y. Wei

[e]School of Physics and Materials Engineering, Hefei Normal University, Anhui Hefei, 230601, China

Corresponding Authors E-mail: xbzhu@issp.ac.cn; bchzhao@issp.ac.cn

‡ These authors contributed equally to this work.

Experimental section

Materials synthesis: Firstly, the $NiMoO_4$ precusor material was synthesized by a simple one-pot hydrothermal process. In detail, 0.25 g glucose was uniformly dispersed in 60 ml DI water under continuous stirring for 0.5 h. Then, 0.8724 g $Ni(NO_3)_2 \cdot 6H_2O$, 0.5297 g $(NH_4)_6Mo_7O_{24} \cdot 4H_2O$ and 1.4019 g hexamethylenetetramine were dissolved in the above solution and stirred for 1h. Next, the mixed solution was transferred to a 100 ml Teflon-lined stainless steel autoclave and kept temperature at 200 °C for 24 h. After cooling to room temperature, the brown sediment was washed several times by centrifugation using DI water and ethanol, and dried under a vacuum at 60 °C for 12 h. Secondly, the sulfur powder and the obtained $NiMoO_4$ precusor were put at the upstream and downstream of the tube furnace, respectively, and annealed at 500 °C for 2 h under H_2/Ar atmosphere to obtain the final MoS_2/Ni_3S_2@C material. For comparison, Ni_3S_2/C, MoS_2/C and MoS_2/Ni_3S_2 materials were also synthesized via the similar process just without Mo or Ni sources or glucose additives.

Materials characterizations: The phase purity and structure of the obtained materials were verfied by X-ray diffraction (XRD) with Cu Kα radiation. The morphology and microstructure were probed by the scaning electron microscopy (SEM, SU 8020, HITACHI), transmission electron microscopy (TEM, Tecnai G2F20), and high-resolution transmission electron microscopy (HRTEM). The elemental mapping measurement was carried out in the energy-dispersive X-ray spectroscope (EDS) attached to TEM. Raman spectroscopy measurements were performed on a Horiba Jobin Yvon T6400 with a 514.5 nm laser excitation. X-ray photoelectron spectroscopy (XPS) was collected by a Thermo Scientific ESCALAB 250 with Al Kα as the excitation source. The specific surface area and pore size distribution were provided by N_2 adsorption and desorption test (Autosorb-iQ-Cx) at 77 K using the Bruauer-Emmett-Teller (BET) and Barret-Joyner-Halenda (BJH) methods. Thermogravimetric analysis (TGA) was implemented by the Pyris 1 Thermogravimetric Analyzer. The electrical conductivity measurements were carried out on a commercial Physical Property Measurement System (PPMS, 1.8 K≤T≤400 K, 0 T≤H≤9 T) using the four-probe

method.

Electrochemical measurements: Electrochemical performance was evaluated using CR2032 coin-type cells, which were assembled in an argon-filled glove box with moisture and oxygen less than 0.1 ppm. The working electrode was prepared by mixing the as-prepared materials, Super P, and sodium carboxymethyl cellulose (CMC) in a weight ratio of 7:2:1 into a certain amount of DI water. The uniformly mixed slurry was pasted onto Cu foil and then dried in a vacuum oven at 80 °C overnight. The loading mass of the working electrodes is about 1-2 mg/cm^2. For SIBs, Na foil was employed as the counter electrode, glass microfiber filters as the separator, and 1 M $NaClO_4$ dissolved in PC (propylene carbonate) and EC in a volume ratio of 1:1 with 5% FEC (fluoroethylene carbonate) as the electrolyte. For PIBs, K foil was served as the counter electrode, glass microfiber filters as the separator, and 3 M KFSI in DME (1, 2-Dimethoxyethane) as the electrolyte. Galvanostatic charge and discharge (GCD) measurements were carried out on a LAND battery test system in a voltage window of 0.01-3.0 V. Cyclic voltammetry (CV) measurements from 0.01 to 3.0 V at different scan rates and electrochemical impendence spectra (EIS) at the frequency range of 10^5-0.01 Hz were performed using a CHI 660E electrochemical workstation.

DFT Calculation: The density functional theory (DFT) calculations were performed by the Vienna Ab-initio Simulation Package (VASP).[1] According to the generalized gradient approximation (GGA), the projector-augmented wave (PAW) pseudopotential with Perdew-Burke-Ernzerhof (PBE) parametrization were used.[2] The cut-off energy for the wave function is set as 450 eV, and the Brillouin zone was sampled via a Γ-centered *k*-mesh scheme with a 0.02 × 2π Å^{-1} space. The energy and force were converged to 1.0×10^{-5} eV/atom and 0.02 eV/ Å, respectively. A 20 Å vacuum layer thickness was applied to avoid virtual interaction. The adsorption energy of Na on MoS_2 or MoS_2/Ni_3S_2 heterostructure was calculated by $E_{ads}=E_{total}-E_{Na}-E_{host}$, where the E_{total} is the total energy of Na-absorbed MoS_2 or MoS_2/Ni_3S_2 heterostructure, E_{Na} is the energy of isolated Na atom and E_{host} is the energy of MoS_2 or MoS_2/Ni_3S_2 heterostructure framework.

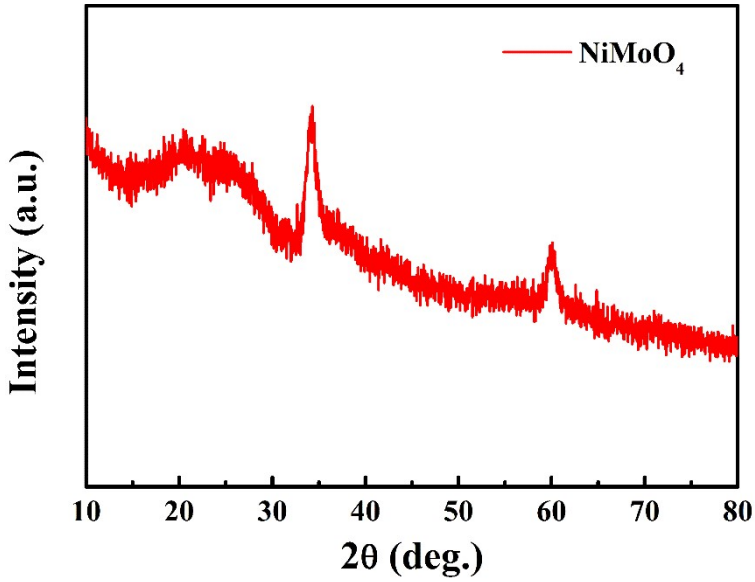

Fig. S1. XRD pattern of the $NiMoO_4$ precursor material.

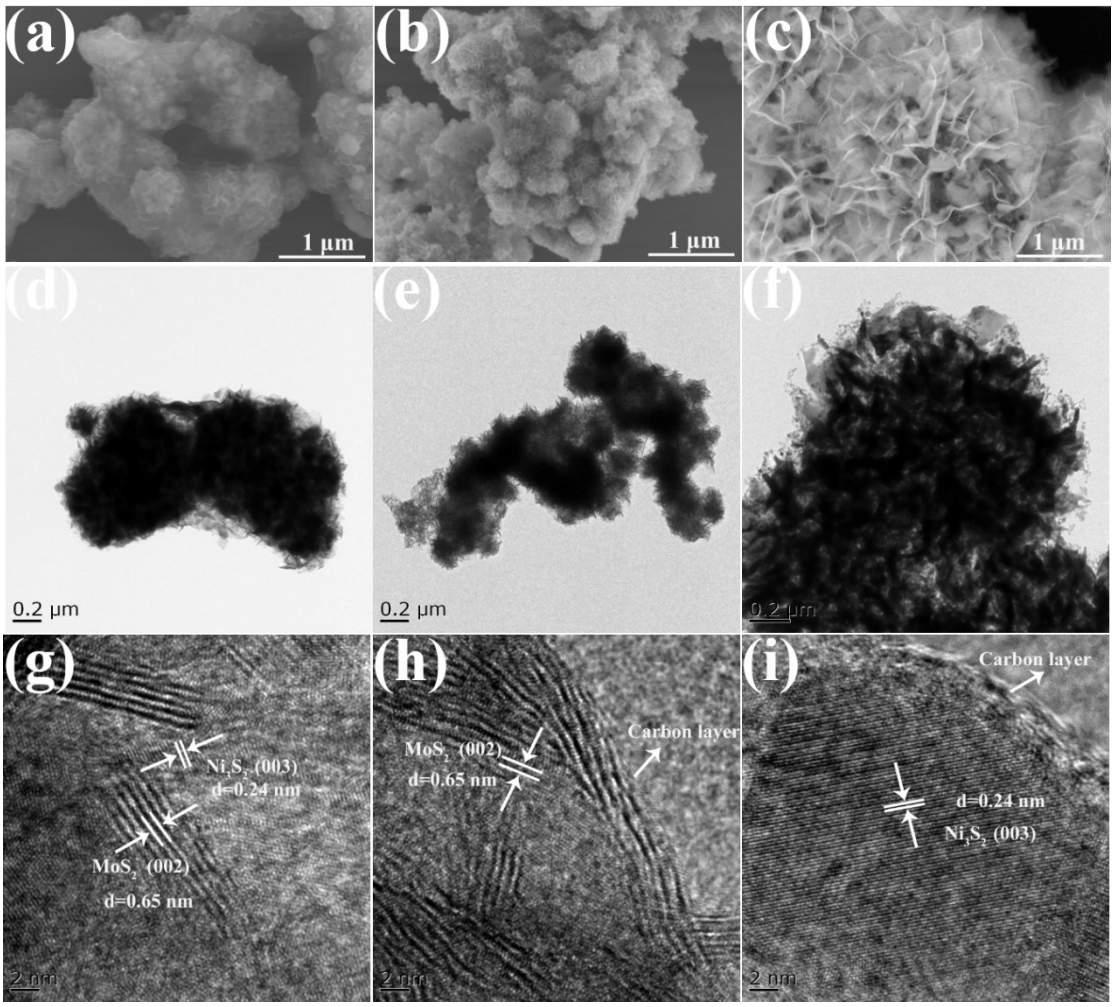

Fig. S2. a-c) SEM, d-f) TEM and g-i) HRTEM images of the MoS_2/Ni_3S_2, MoS_2/C and Ni_3S_2/C samples.

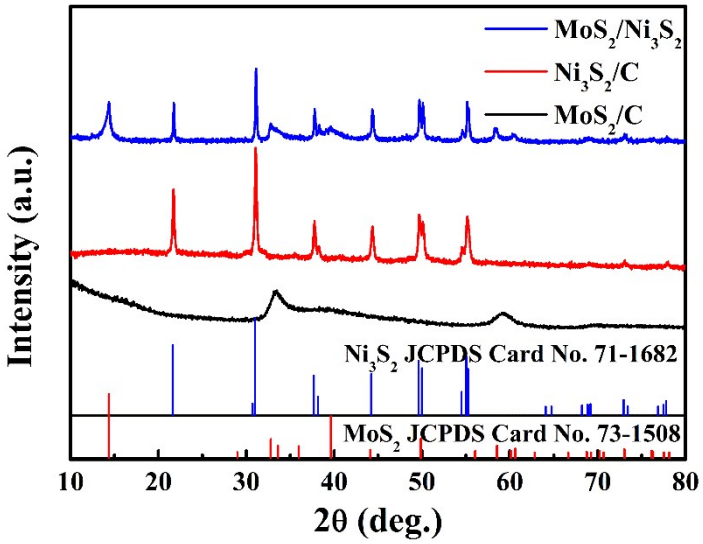

Fig. S3. XRD patterns of the MoS_2/Ni_3S_2, MoS_2/C and Ni_3S_2/C samples.

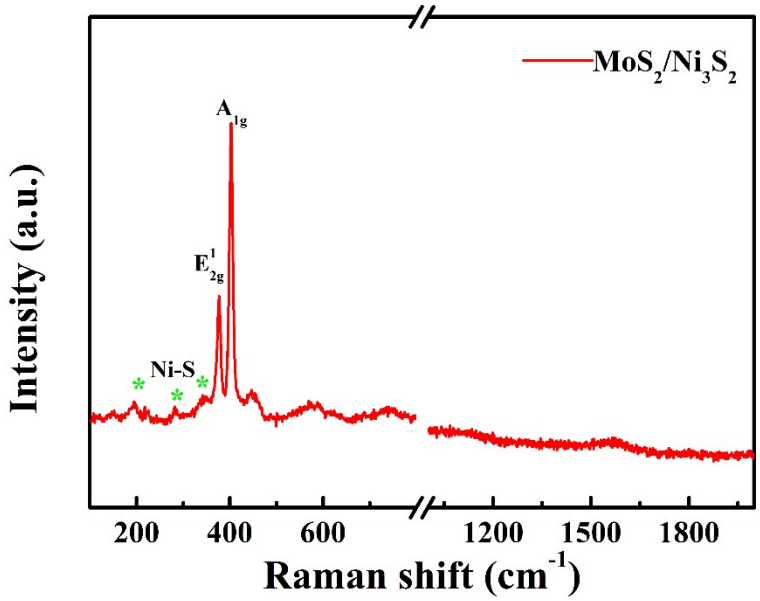

Fig. S4. Raman spectrum of the MoS_2/Ni_3S_2 sample.

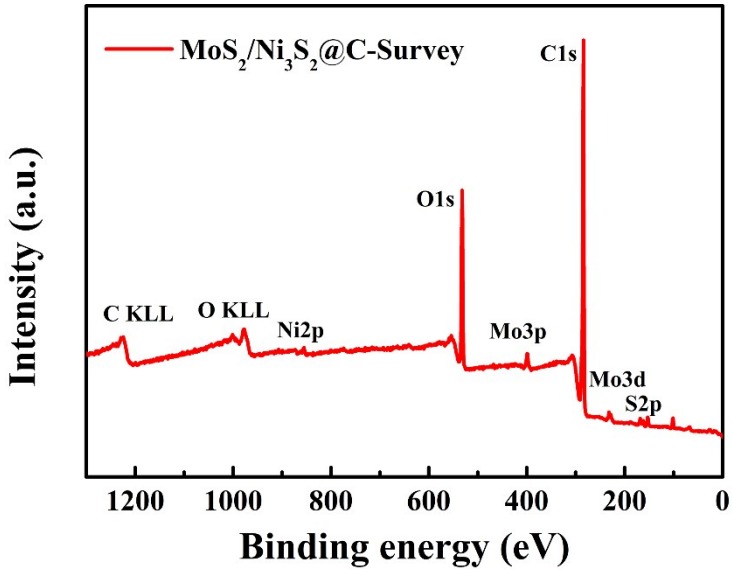

Fig. S5. XPS survey spectrum the MoS_2/Ni_3S_2@C material.

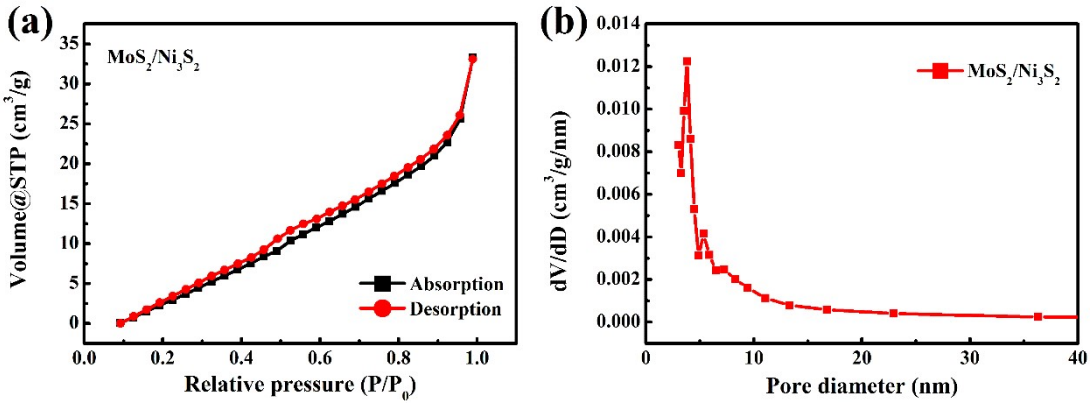

Fig. S6. a) Isothermal N_2 adsorption and desorption curves and b) pore size distribution of the MoS_2/Ni_3S_2 sample.

Detailed process about TGA calculation of the MoS_2/Ni_3S_2@C sample: In the temperature range from 50 to 700 °C in air, the main part of the weight loss is composed of three parts: the oxidation of MoS_2, Ni_3S_2 and carbon layer. The total weight loss is about 46.5 wt.% in the experimental process. Assumed to the final product is MoO_3 and NiO, the corresponding reaction equations can be written as follows:

$$2MoS_2 + 7O_2 \rightarrow 2MoO_3 + 4SO_2 \quad (1)$$

$$2Ni_3S_2 + 7O_2 \rightarrow 6NiO + 4SO_2 \quad (2)$$

$$C + O_2 \rightarrow CO_2 \quad (3)$$

The carbon content of the Ni_3S_2/MoS_2/C heterostructure material was calculated based on the following procedures:

Assumed to molar mass of MoS_2 = M_1, Ni_3S_2 = M_2, MoO_3 = M_3, NiO = M_4, the total content of the heterostructure material = m_0, the content of MoS_2 in the heterostructure = m_1, Ni_3S_2 content in the heterostructure = m_2, MoO_3 content in the heterostructure = m_3, NiO content in the heterostructure = m_4 and carbon content in the heterostructure = m_5.

Due to the final product is MoO_3 and NiO, so $m_3 + m_4 = 0.535m_0$.

According to Equation (1) and (2), m_3 and m_4 can be deduced from $m_3 = M_3 \times m_1/M_1 = 0.90m_1$, and $m_4 = M_4 \times 3m_2/M_2 = 0.90m_2$, respectively.

Combining the EDS results, the atomic ratio of Ni and Mo is about 2:1, we can calculate that m_1/m_2 is about 1:1. So, we can obtain $0.9m_1 + 0.90m_2 = 0.535m_0$, $m_1 = m_2 = 0.3m_0$,

Thus, carbon content of the heterostructure $m_5 = m_0 - 0.6m_0 = 0.4m_0$.

So, the contents of MoS_2, Ni_3S_2 and carbon in the heterostructure material are about 30

wt%, 30 wt% and 40 wt%, respectively.

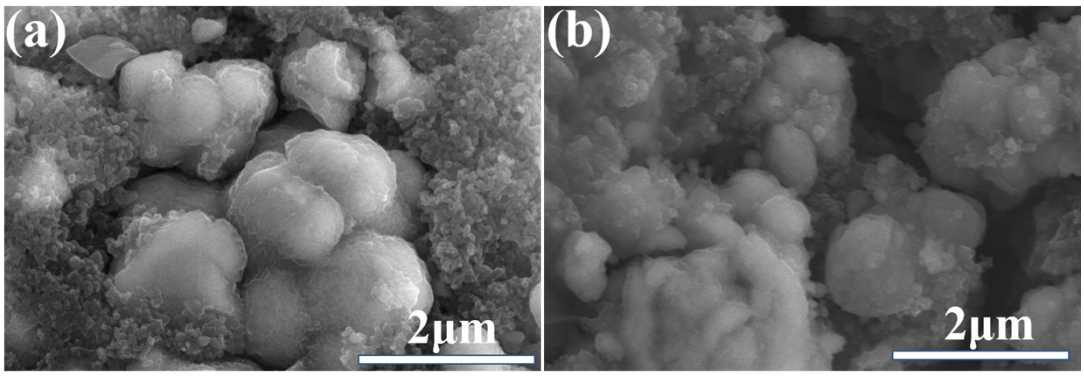

Fig. S7. The SEM images of (a) before cycling and (b) after 200 cycles for the MoS_2/Ni_3S_2@C electrode for SIBs.

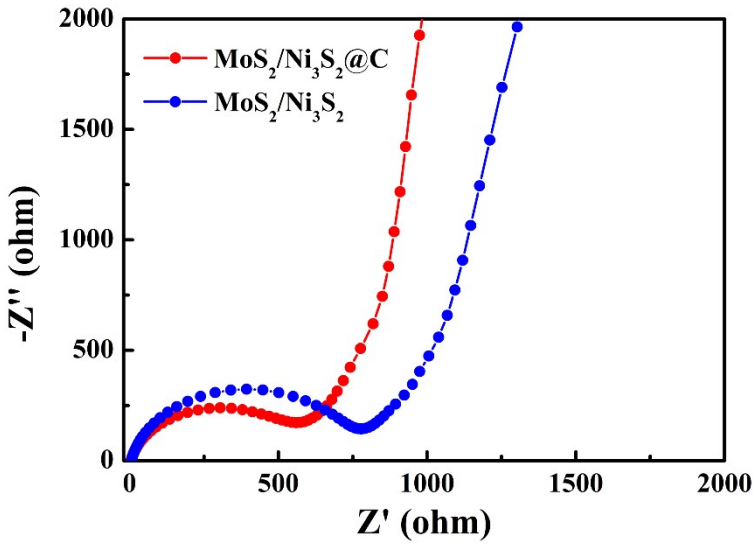

Fig. S8. EIS comparison of the for the MoS_2/Ni_3S_2@C and MoS_2/Ni_3S_2 electrodes for SIBs.

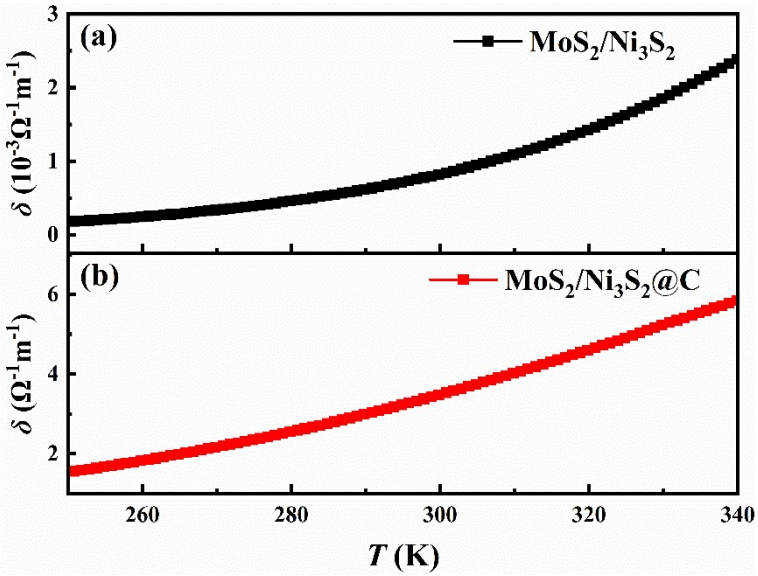

Fig. S9. The relationship of temperature dependent electrical conductivity at the range of 250-340 K for (a) MoS_2/Ni_3S_2 and (b) MoS_2/Ni_3S_2@C electrodes.

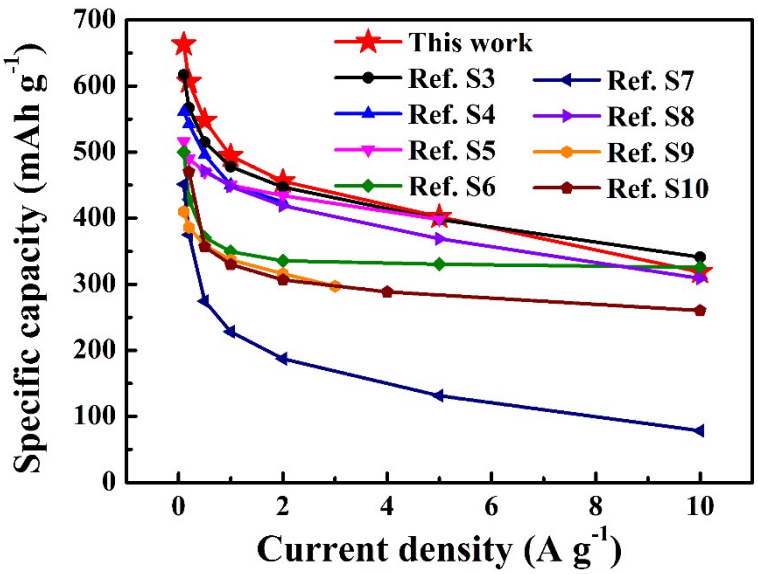

Fig. S10. Rate performance comparison of this work with the previously reported MoS_2-based heterostructure anodes for SIBs.

Table S1 The detailed comparison of the sodium storage performance this work with the previously reported MoS_2-based heterostructure anodes for SIBs.

Electrodes	**Cycling performance ($mAh\ g^{-1}/n/A\ g^{-1}$)**	**Rate performance ($mAh\ g^{-1}/A\ g^{-1}$)**	**Loading mass ($mg\ cm^{-2}$)**	**Ref.**
Bi_2S_3/MoS_2	427.7/100/0.5	325.5/10	1.0-1.2	[6]
$MnS\text{-}MoS_2$	214/500/1.0	78.3/10	1.2	[7]
NB-NiMoS	420/200/0.5	309/10	1.4	[8]
Cu_2S@carbon@MoS_2	300/200/0.3	297/3	1.0	[9]
MoS_2-NiS	391/700/2.0	342/10	1.5	[3]
$G/NiS_2\text{-}MoS_2$	509.6/500/0.5	424.5/2	1.0	[4]
Cu_2S/MoS_2⊂Carbon	336.2/300/1.0	260.2/10	1.0	[10]
$NiS/MoS_2/C$	335/190/1.0	398/5	1.0-2.0	[5]
MoS_2/Ni_3S_2@C	**400/200/1.0**	**318.5/10**	**1.0-2.0**	**This work**

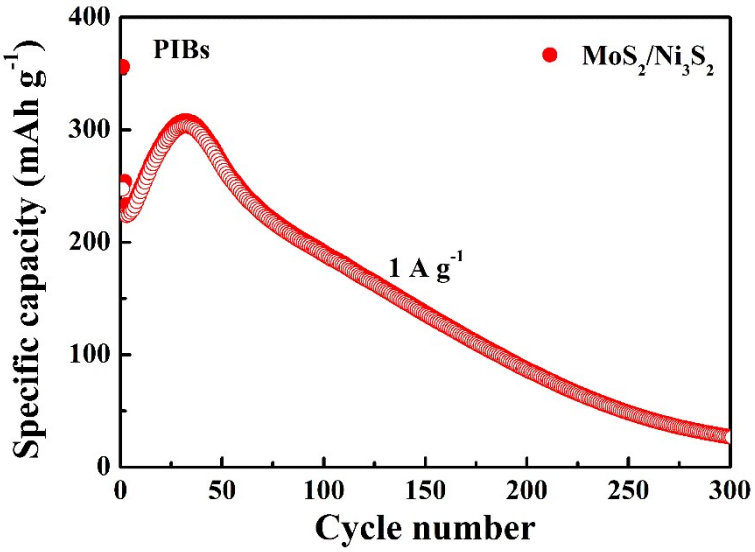

Fig. S11. The cycling performance of the MoS_2/Ni_3S_2 electrode for PIBs at 1 A g^{-1}.

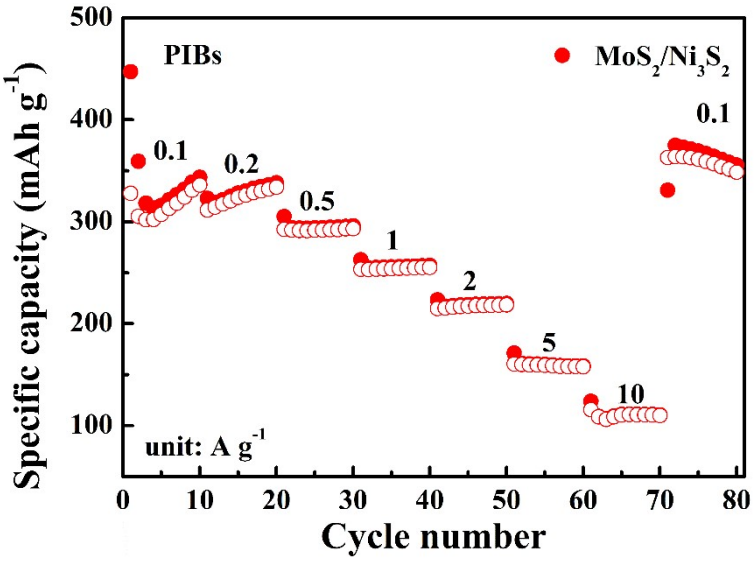

Fig. S12. The rate performance of the MoS_2/Ni_3S_2 electrode for PIBs.

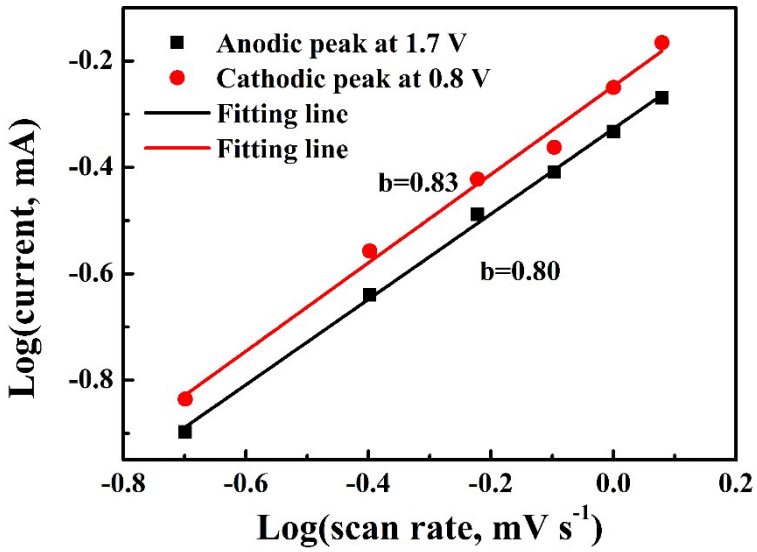

Fig. S13. The fitted *b* values at the different redox peaks for the MoS_2/Ni_3S_2@C heterostructure electrode in SIBs.

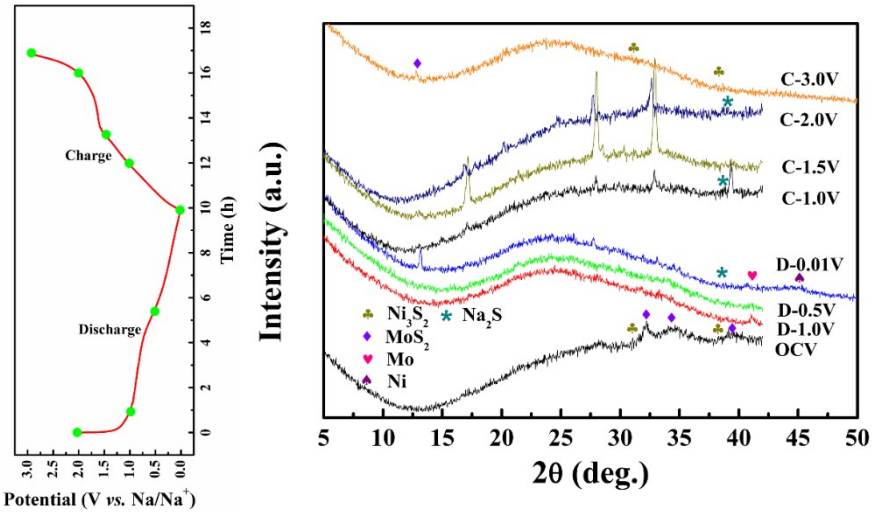

Fig. S14. *Ex-situ* XRD patterns of the MoS_2/Ni_3S_2@C heterostructure electrode for SIBs at the different discharge/charge states.

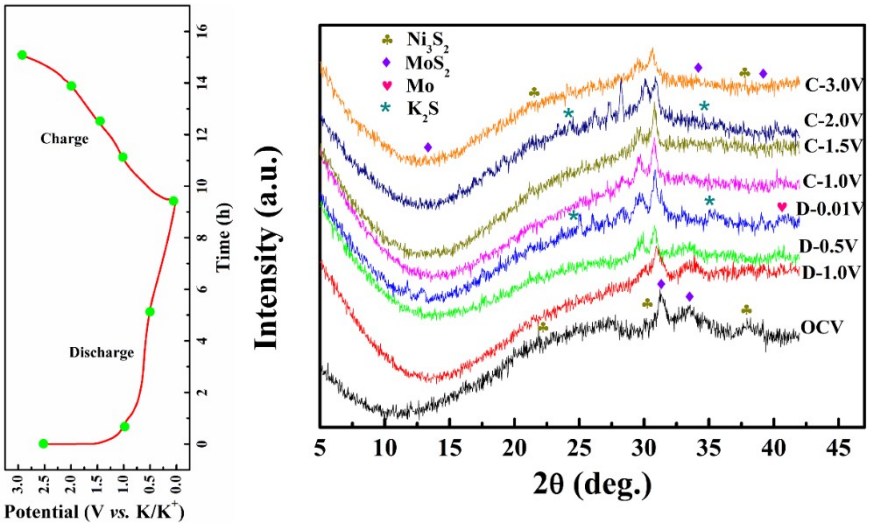

Fig. S15. *Ex-situ* XRD patterns of the MoS_2/Ni_3S_2@C heterostructure electrode for PIBs at the different discharge/charge states.

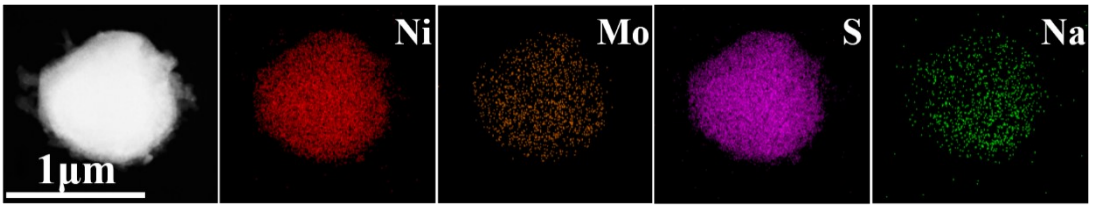

Fig. S16. EDS-mapping images of the MoS_2/Ni_3S_2@C electrode heterostructure electrode for SIBs at the full de-sodiation state.

Fig. S17. EDS-mapping images of the MoS_2/Ni_3S_2@C electrode heterostructure electrode for PIBs at the full de-potassiation state.

References

[1] Kresse, G.; Furthmüller, J., Efficiency of ab-initio total energy calculations for metals and semiconductors using a plane-wave basis set. *Compos. Mater. Sci.* **1996**, *6*, 15-50.

[2] Perdew, J.P.; Burke, K.; Ernzerhof, M., Generalized Gradient Approximation Made Simple. *Phys. Rev. Lett.* **1996**, *77*, 3865-3868.

[3] Yang, F.; Wang, S.; Guan, J.; Shao, L.; Shi, X.; Cai, J.; Sun, Z., Hierarchical MoS_2-NiS nanosheet-based nanotubes@N-doped carbon coupled with ether-based electrolytes towards high-performance Na-ion batteries. *J. Mater. Chem. A* **2021**, *9*, 27072-27083.

[4] Huang, J.; Yao, Y.; Huang, M.; Zhang, Y.; Xie, Y.; Li, M.; Yang, L.; Wei, X.; Li, Z., Creating Unidirectional Fast Ion Diffusion Channels in G/NiS_2-MoS_2 Heterostructures for High-Performance Sodium-Ion Batteries. *Small* **2022**, *18*,

2200782.

[5] Xie, H.; Chen, M.; Wu, L., Hierarchical Nanostructured NiS/MoS_2/C Composite Hollow Spheres for High Performance Sodium-Ion Storage Performance. *ACS Appl. Mater. Interfaces* **2019,** *11*, 41222-41228.

[6]. Cao, L.; Liang, X.; Ou, X.; Yang, X.; Li, Y.; Yang, C.; Lin, Z.; Liu, M., Heterointerface Engineering of Hierarchical Bi_2S_3/MoS_2 with Self-Generated Rich Phase Boundaries for Superior Sodium Storage Performance. *Adv. Funct. Mater.* **2020**, *30*, 1910732.

[7] Chen, F.; Shi, D.; Yang, M.; Jiang, H.; Shao, Y.; Wang, S.; Zhang, B.; Shen, J.; Wu, Y.; Hao, X., Novel Designed MnS-MoS_2 Heterostructure for Fast and Stable Li/Na Storage: Insights into the Advanced Mechanism Attributed to Phase Engineering. *Adv. Funct. Mater.* **2020**, *31*, 2007132.

[8] Choi, J. H.; Park, S.-K.; Kang, Y. C., N-Doped Carbon Coated Ni-Mo Sulfide Tubular Structure Decorated with Nanobubbles for Enhanced Sodium Storage Performance. *Chem. Eng. J.* **2020**, *383*, 123112.

[9] Fang, Y.; Luan, D.; Chen, Y.; Gao, S.; Lou, X. W. D., Rationally Designed Three-Layered Cu_2S@Carbon@MoS_2 Hierarchical Nanoboxes for Efficient Sodium Storage. *Angew. Chem., Int. Ed.* **2020**, *59*, 7178-7183.

[10] Shi, N.; Xi, B.; Huang, M.; Ma, X.; Li, H.; Feng, J.; Xiong, S., Hierarchical Octahedra Constructed by Cu_2S/MoS_2⊂Carbon Framework with Enhanced Sodium Storage. *Small* **2020**, *16*, 2000952.